

Electronic Structure of Graphene Grown on a Hydrogen-terminated Ge (110) Wafer

Sung Joon AHN,* Hyun Woo KIM, Ishwor Bahadur KHADKA, Krishna Bahadur RAI and Joung Real AHN†
*Department of Physics, Sungkyunkwan University, Suwon 16419, Korea and
SAINT, Sungkyunkwan University, Suwon 16419, Korea*

Jae-Hyun LEE*
*Department of Energy Systems Research and Department of Materials
Science and Engineering, Ajou University, Suwon 16499, Korea*

Seog Gyun KANG and Dongmok WHANG
*School of Advanced Materials Science and Engineering,
Sungkyunkwan University, Suwon 16419, Korea and
SAINT, Sungkyunkwan University, Suwon 16419, Korea*

(Received 11 May 2018, in final form 20 June 2018)

Using angle-resolved photoemission spectroscopy, we studied the electronic structure of graphene grown on a Ge (110) wafer, where a single-crystal single-layer graphene was recently grown using chemical vapor deposition. The growth mechanism of the single-layer single-crystal graphene was related to the hydrogen termination of the Ge (110) surface. To further understand the growth mechanism, we measured the electronic structure of the graphene-covered Ge (110) wafer in a vacuum as a function of the increasing temperature, which led to a deintercalation of the hydrogen atoms. Furthermore, we measured the electronic structure after the reintercalation of the hydrogen atoms between the Ge substrate and graphene. These findings show that hydrogen is intercalated between the Ge substrate and graphene after the growth of graphene using chemical vapor deposition.

PACS numbers: 79.60.-i, 81.05.ue, 71.20.-b, 68.43.-h

Keywords: Graphene, Angle-resolved photoemission spectroscopy, Chemical vapor deposition

DOI: 10.3938/jkps.73.656

I. INTRODUCTION

Two-dimensional (2D) materials such as graphene, transition-metal dichalcogenides, and black phosphorene exhibit very promising physical properties for applications in electronic devices. The development of various methods to achieve a high-quality large-scale fabrication of these materials has been of key importance [1–8]. For graphene, some of the fabrication methods are based on mechanical exfoliation of graphite. High-quality graphene has been deposited on metal foils using the chemical vapor deposition (CVD) method [1,2,9] and fabricated on crystal surfaces such as 6H-SiC (0001), Ru (0001), and Ir (111) using epitaxial growth [10–14]. The CVD fabricated graphene on metal foils can be employed for the development of electronic devices; this fabrication

method has various advantages including simple transfer, low growth temperature, and low cost [1,9]. Although the CVD-grown graphene on metal foils is polycrystalline, its quality has been improved by the reduction of the density of graphene seeds on metal foils [1,3,15,16]. Various transfer methods have been reported including the wet transfer (*e.g.*, chemical etching), dry transfer (using thermal release tapes or metal films), and bubbling transfer schemes [1,17–19].

After the fabrication of single-crystal graphene on a hydrogen-terminated Ge-(110)-surface using CVD, the paradigm of CVD-grown graphene changed [4]. Instead of the reduction of the seed density, unidirectionally aligned graphene seeds originating from an anisotropic substrate and graphene stitching without zero-angle grain boundaries provided a new paradigm of single-crystal graphene growth. In addition, dry-transfer of graphene single-crystals grown on Ge substrates is attainable owing to the weak chemical interactions between graphene and hydrogen-terminated Ge substrate. Dur-

*Sung Joon Ahn and Jae-Hyun Lee contributed equally to this work.

†E-mail: jrahn@skku.edu

ing the CVD growth, hydrogen was reported to restrict the etching processes owing to the oxygen impurities. The step-edge structures of the hydrogen-terminated Ge substrate were suggested to contribute to the formation of graphene single crystals [20, 21]. However, the research findings on the existence of hydrogen atoms in the graphene-covered Ge substrate are insufficient and inconclusive [4, 22, 23].

In this study, using angle-resolved photoemission spectroscopy (ARPES) and low-energy electron diffraction (LEED), we provide an evidence that supports the hypothesis that hydrogen atoms are intercalated between the CVD-grown graphene and Ge substrate. We performed experimental deintercalation and reintercalation processes of the hydrogen atoms, and showed that the electronic structure and diffraction pattern of the graphene-covered Ge surface was fully recovered after these processes, which suggests the existence of hydrogen atoms between the CVD-grown graphene and Ge substrate.

II. EXPERIMENTS AND DISCUSSION

First, as a pretreatment, we removed the surface germanium-oxide layers and organic contaminants. A Ge wafer was cleaned by the standard Radio Corporation of America (RCA) cleaning process, followed by an oxygen-plasma treatment [24]. The Ge wafer was dipped into a 10% hydrofluoric acid solution to remove the surface germanium-oxides, which passivated the Ge surface's dangling bonds with hydrogen atoms. The hydrogen-terminated Ge wafer was loaded into a low-pressure CVD chamber. The chamber was pumped down to a pressure of 10^{-5} Torr to avoid the formation of surface oxides. After the pumping, we started to introduce H_2 gas (99.999% purity) into the chamber, and increased the temperature to 910 °C. When the optimal temperature was reached, a hydrogen-plasma treatment was applied for 10 min to remove the unavoidable surface oxides. For the synthesis of graphene, a gas mixture of H_2 and CH_4 (100 : 1 ratio) was introduced in the chamber, and a total pressure of 100 Torr was maintained for 2 h. Then, the sample was rapidly cooled to room temperature in vacuum [4].

After loading the sample into the ultra-high-vacuum chamber, it was heated to 925 °C to remove residues and deintercalate the hydrogen atoms between the CVD-grown graphene and Ge substrate. After the deintercalation, we performed an ex-situ hydrogen intercalation. The crystalline and electronic band structures of the CVD-grown graphene during the deintercalation and reintercalation processes were measured using LEED and ARPES, respectively. The ARPES spectra were measured with a commercial angle-resolved photoelectron spectrometer (R3000, VG-Scienta) and monochromated He-II radiation beam source (VG-Scienta) at

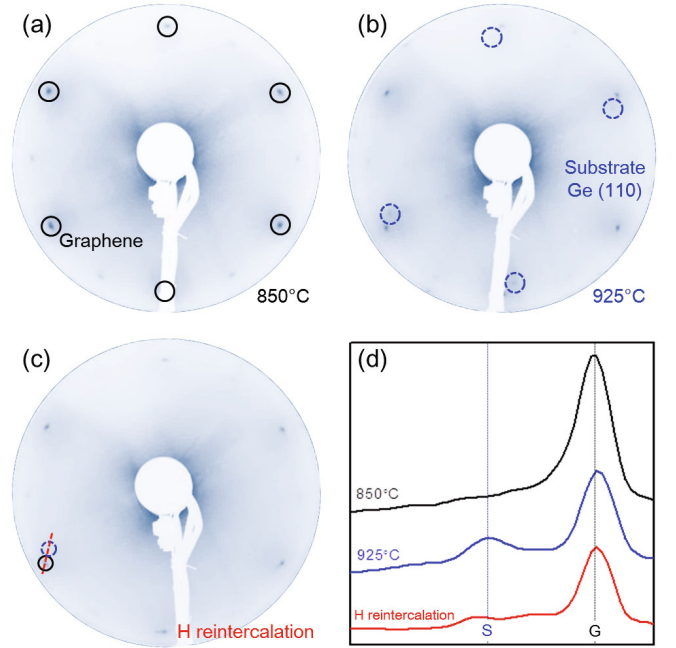


Fig. 1. (Color online) Experimental LEED data of the CVD-grown graphene on the hydrogen-terminated Ge (110) substrate, with a beam energy of 80 eV. (a) LEED pattern after the heating to 850 °C, where the LEED peaks of graphene are indicated by the black circles. (b) LEED pattern after the heating to 925 °C, where the LEED peaks of Ge (110) are indicated by the blue dashed circles. (c) LEED pattern after the reintercalation of the hydrogen atoms. (d) Line profiles near an LEED peak of graphene, obtained along the red dashed line in (c), where the peaks labeled as G and S originate from graphene and Ge (110), respectively.

room temperature. As described in Ref. 4, single-oriented graphene seeds are grown along the specific direction, $[\bar{1}10]$, of the hydrogen-terminated Ge(110) surface. The single-oriented graphene seeds coalesce into single-crystal graphene, where the positions of the single-oriented graphene seeds can be adjusted during the coalescence [4].

Figure 1 shows the changes in the LEED patterns of the CVD-grown graphene on the hydrogen-terminated Ge (110) substrate during the deintercalation and reintercalation of the hydrogen atoms; the LEED beam energy was 80 eV. Figure 1(a) shows the LEED pattern after the heating to 850 °C, where the LEED peaks of graphene appear, as indicated by the black circles; the LEED peaks of the Ge substrate are not visible [4]. Above a heating temperature of 900 °C, the LEED peaks of the Ge (110) substrate became visible, as indicated by the blue-dashed circles in Fig. 1(b). The appearance of the LEED pattern of the Ge substrate suggests that the hydrogen atoms begin to be deintercalated above 900 °C. The deintercalation temperature of the hydrogen atoms is similar to that of 6H-SiC (0001). When a 6H-SiC (0001) substrate without

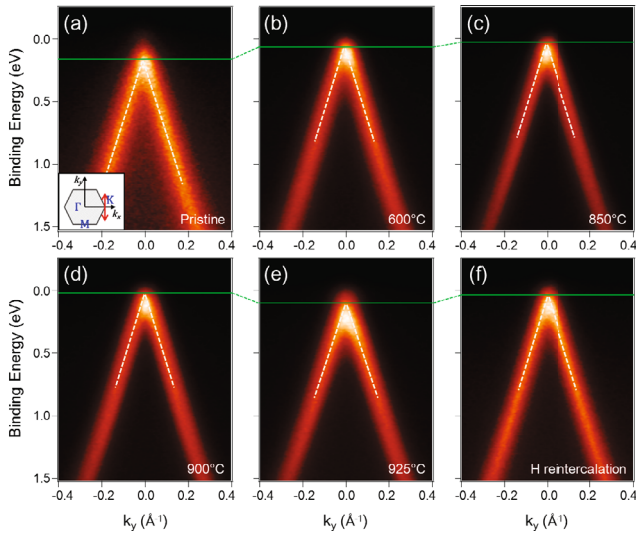


Fig. 2. (Color online) Changes in the ARPES intensity maps of the CVD-grown graphene on the hydrogen-terminated Ge (110) substrate near the K-point (see the inset in (a)). (a) ARPES intensity map of the as-grown graphene. (b) - (e) ARPES intensity maps measured after the heating to (b) 600 °C, (c) 850 °C, (d) 900 °C, and (e) 925 °C, respectively. (f) ARPES intensity map measured after the reintercalation of the hydrogen atoms. The Dirac-point energies in (a) - (f) are indicated by the green lines.

graphene is terminated with hydrogen atoms, the desorption temperature of the hydrogen atoms is approximately 590 °C, whereas that of a Ge substrate with graphene is 300 °C [25–27]. When hydrogen atoms are intercalated between the epitaxial graphene and SiC substrate, the desorption temperature increases to approximately 900 °C [28]. After the deintercalation, the hydrogen atoms were reintercalated in another vacuum chamber under a hydrogen pressure of 750 Torr at 900 °C. Subsequently, the graphene-covered Ge substrate was placed again in the analysis chamber [28]. The presence of dangling bonds make the surface reactive, resulting in dissociative adsorption of hydrogen molecules on the surface [29–31]. Accordingly, the temperatures of hydrogen intercalation between the graphene and the SiC (0001) surface were between 550 and 1000 °C, which is significantly lower than the thermal decomposition temperature of hydrogen molecules [28,32,33]. Figure 1(c) shows the LEED pattern after the reintercalation, where the LEED peaks of the Ge substrate disappeared again; only the graphene peaks were observed. The line-profile in Fig. 1(d) was also recovered, where the peaks labeled as G and S originated from the CVD-grown graphene and Ge substrate, respectively. The LEED patterns suggest that hydrogen atoms were intercalated between the CVD-grown graphene and Ge substrate during the CVD growth.

In addition, we measured ARPES intensity maps during the deintercalation and reintercalation, as shown in Fig. 2. These maps were measured along the direc-

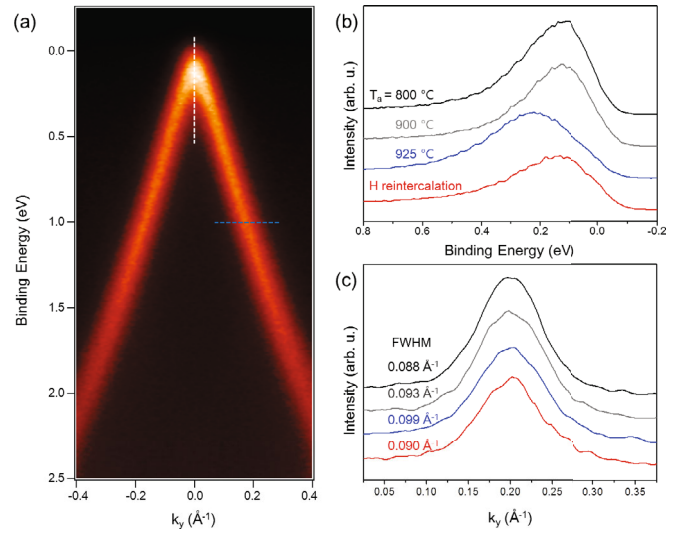


Fig. 3. (Color online) (a) ARPES intensity map measured after the reintercalation of the hydrogen atoms. (b) Changes in EDCs. (c) Changes in MDCs. The EDCs and MDCs were obtained along the white and blue dashed lines in (a), respectively. In (b) and (c), the black, grey, blue, and red lines correspond to data measured after the heating to 800 °C, 900 °C, and 925 °C, and after reintercalation of the hydrogen atoms, respectively.

tion perpendicular to the Γ -K direction across the K point, as shown in the inset of Fig. 2(a), where the K-point is located at $k_y = 0 \text{ \AA}^{-1}$. Figure 2(a) shows the ARPES intensity map before the deintercalation, which reveals that the Dirac-point energy is 0.163 eV, and suggests that the CVD-grown graphene is electron-doped. However, the electron doping is not intrinsic and originates from the inevitable chemical residues formed during the CVD growth or when the sample was exposed to air. The electron doping can be understood through the following thermal treatments. When the graphene-covered Ge substrate was heated from 600 °C to 850 °C, the Dirac-point energy decreased to 0.022 eV, making graphene almost neutral, as shown in Fig. 2(d). This decrease of the Dirac-point energy suggests that the chemical residues were removed. However, when the graphene-covered wafer was heated further, above 900 °C, the Dirac-point energy increased to 0.102 eV, as shown in Fig. 2(e). The increase of the Dirac-point energy suggests that hydrogen atoms intercalated between the CVD-grown graphene, and that the Ge substrate became deintercalated [34]. After the deintercalation of the hydrogen atoms, graphene partially bonds to Ge atoms on the Ge surface. As electrons are transferred from the dangling bonds of the Ge atoms to graphene, as reported previously, the increase of the Dirac-point energy is consistent with the suggestion that graphene becomes electron-doped [35,36]. The clear observation of the Dirac-cone of graphene on the Ge surface without hydrogen atoms is different from that on a SiC surface [11,28], where graphene is insulating and exhibits

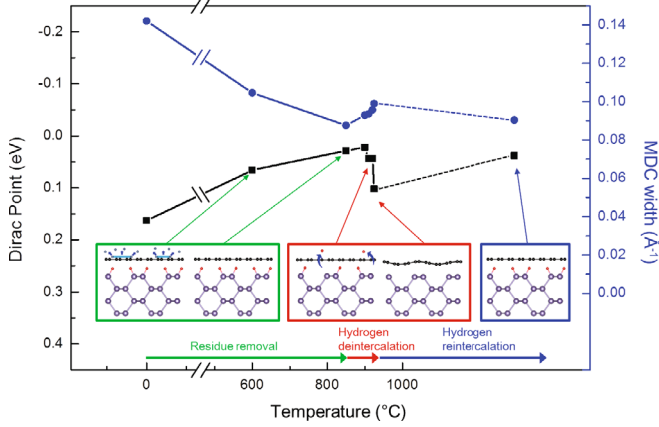


Fig. 4. (Color online) Changes in Dirac-point energies (black) and FWHMs (blue) of the MDCs after the heating and reintercalation of the hydrogen atoms. The insets show atomic-structure models during the heating, deintercalation, and reintercalation; the black, purple, and red atoms correspond to Ge, graphene, and hydrogen, respectively.

only flat bands. The clear observation of the Dirac-cone suggests that graphene weakly bonds to Ge atoms on the Ge surface, compared to the stronger bonds between Si atoms on a SiC surface and graphene [28]. Recent scanning tunneling microscopy (STM) and ARPES experiments and density functional theory (DFT) calculations of graphene grown on a Ge(110) surface also support that interactions between graphene and a Ge surface are weak, where graphene was grown directly on a clean Ge(110) surface in vacuum so that it is located directly on a clean Ge(110) surface [37]. When the hydrogen atoms are reintercalated in the other vacuum chamber, the Dirac-point energy changed to 0.038 eV, as shown in Fig. 2(f), and graphene became almost neutral again. This implies that the Ge surface is fully saturated with hydrogen atoms. The Dirac-point energy after the reintercalation is very similar to that measured after the removal of the chemical residues, as shown in Figs. 2(d) and 2(f). The deintercalation and reintercalation results suggest that the hydrogen atoms are intercalated between the CVD-grown graphene and Ge substrate.

We further analyzed the ARPES spectra, and studied the energy distribution curves (EDCs) and momentum distribution curves (MDCs) as well as their changes during the deintercalation and reintercalation of hydrogen atoms, as shown in Fig. 3. The EDCs in the figure are plotted along the energy direction at the K point, while the MDCs are plotted along the momentum direction at a binding energy of 1 eV. Figure 3(b) shows that, as described above, the Dirac-point energy increases for temperatures above 900 °C owing to the hydrogen deintercalation, and it decreases after the hydrogen reintercalation. In Fig. 3(c), the full-width-at-half-maximum (FWHM) of the MDC after the heating to 800 °C is 0.088 Å⁻¹. The FWHM widens to 0.099 Å⁻¹ with the increase of the heating temperature, which suggests that

the FWHM increases during the hydrogen deintercalation. After the reintercalation of the hydrogen atoms, the FWHM narrows and becomes similar to that measured after the heating to 800 °C. The FWHM can be affected by chemical residues, and roughness and domain size of graphene. As the same graphene layer was used during the deintercalation and reintercalation, the change in FWHM is not related with the domain size of graphene. The presence of a high amount of chemical residues can lead to a widened FWHM. In the present experiments, chemical residues were removed at high heating temperatures; therefore, the widening of the FWHM at high heating temperatures cannot be attributed to chemical residues. Therefore, the change in FWHM originates from the roughness of graphene [38–40], which is related to the bonds between graphene and Ge surface. When graphene is located on a hydrogen-terminated surface, it is relatively flat as there is no external strain. However, when graphene bonds directly to Ge atoms on the surface, it can deform and become rougher. Therefore, the change in FWHM further supports the hypothesis that hydrogen atoms are intercalated between the CVD-grown graphene and Ge wafer.

III. CONCLUSION

As shown in Fig. 4, when the graphene-covered Ge substrate, synthesized using CVD, was heated to 900 °C, the residues were removed. The removal of the residues made the CVD-grown graphene nearly neutral, as the existence of residues contributes to the electron doping. Above 900 °C, the hydrogen atoms between graphene and Ge substrate began to deintercalate, making graphene an electron-doped layer, where electrons were provided by the Ge atoms from the Ge surface. When the hydrogen atoms were reintercalated, the neutral graphene was recovered. Furthermore, the FWHM of the MDC was fully recovered. Therefore, the present ARPES and LEED experiments support the hypothesis that hydrogen atoms were intercalated between the CVD-grown graphene and Ge substrate.

ACKNOWLEDGMENTS

This study was supported by the National Research Foundation of Korea through the grants: NRF-2017M2A2A6A01019384.

REFERENCES

- [1] X. Li, W. Cai, J. An, S. Kim, J. Nah, D. Yang, R. Piner, A. Velamakanni, I. Jung, E. Tutuc, S. K. Banerjee, L. Colombo and R. S. Ruoff, *Science* **324**, 1312 (2009).

- [2] X. Li, C. W. Magnuson, A. Venugopal, J. An, J. W. Suk, B. Han, M. Borysiak, W. Cai, A. Velamakanni, Y. Zhu, L. Fu, E. M. Vogel, E. Voelkl, L. Colombo and R. S. Ruoff, *Nano Lett.* **10**, 4328 (2010).
- [3] N. Petrone, C. R. Dean, I. Meric, A. M. van der Zande, P. Y. Huang, L. Wang, D. Muller, K. L. Shepard and J. Hone, *Nano Lett.* **12**, 2751 (2012).
- [4] J. H. Lee, E. K. Lee, W. J. Joo, Y. Jang, B. S. Kim, J. Y. Lim, S. H. Choi, S. J. Ahn, J. R. Ahn, M. H. Park, C. W. Yang, B. L. Choi, S. W. Hwang and D. Whang, *Science* **344**, 286 (2014).
- [5] Y. H. Lee, X. Q. Zhang, W. Zhang, M. T. Chang, C. T. Lin, K. D. Chang, Y. C. Yu, J. T. Wang, C. S. Chang, L. J. Li and T. W. Lin, *Adv. Mater.* **24**, 2320 (2012).
- [6] Y. Zhan, Z. Liu, S. Najmaei, P. M. Ajayan and J. Lou, *Small* **8**, 966 (2012).
- [7] M. R. Laskar, L. Ma, S. Kannappan, P. S. Park, S. Krishnamoorthy, D. N. Nath, W. Lu, Y. Y. Wu and S. Rajan, *Appl. Phys. Lett.* **102**, 252108 (2013).
- [8] W. Wu, D. De, S. C. Chang, Y. N. Wang, H. B. Peng, J. M. Bao and S. S. Pei, *Appl. Phys. Lett.* **102**, 142106 (2013).
- [9] Q. Yu, J. Lian, S. Siriponglert, H. Li, Y. P. Chen and S-S. Pei, *Appl. Phys. Lett.* **93**, 113103 (2008).
- [10] A. H. Castro Neto, F. Guinea, N. M. R. Peres, K. S. Novoselov and A. K. Geim, *Rev. Mod. Phys.* **81**, 109 (2009).
- [11] C. Riedl, C. Coletti and U. Starke, *J. Phys. D: Appl. Phys.* **43**, 374009 (2010).
- [12] H. Hibino, S. Tanabe, S. Mizuno and H. Kageshima, *J. Phys. D: Appl. Phys.* **45**, 154008 (2012).
- [13] S. Marchini, S. Günther and J. Wintterlin, *Phys. Rev. B* **76**, 075429 (2007).
- [14] J. Coraux, A. T. N'Diaye, C. Busse and T. Michely, *Nano Lett.* **8**, 565 (2008).
- [15] J. Avila, I. Razado, S. Lorcy, R. Fleurier, E. Pichonat, D. Vignaud, X. Wallart and M. C. Asensio, *Sci. Rep.* **3**, 2439 (2013).
- [16] L. Banszerus, M. Schmitz, S. Engels, J. Dauber, M. Oellers, F. Haupt, K. Watanabe, T. Taniguchi, B. Beschoten and C. Stampfer, *Sci. Adv.* **1**, e1500222 (2015).
- [17] J. D. Caldwell, T. J. Anderson, J. C. Culbertson, G. G. Jernigan, K. D. Hobart, F. J. Kub, M. J. Tadjer, J. L. Tedesco, J. K. Hite, M. A. Mastro, R. L. Myers-Ward, C. R. Eddy, P. M. Campbell and D. K. Gaskill, *ACS Nano*, **4**, 1108 (2010).
- [18] J. Kim, H. Park, J. B. Hannon, S. W. Bedell, K. Fogel, D. K. Sadana and C. Dimitrakopoulos, *Science* **342**, 833 (2013).
- [19] L. B. Gao, W. C. Ren, H. L. Xu, L. Jin, Z. X. Wang, T. Ma, L. P. Ma, Z. Y. Zhang, Q. Fu, L. M. Peng, X. H. Bao and H. M. Cheng, *Nat. Commun.* **3**, 699 (2012).
- [20] S. Choubak, P. L. Levesque, E. Gaufres, M. Biron, P. Desjardins and R. Martel, *J. Phys. Chem. C* **118**, 21532 (2014).
- [21] J. Dai, D. Wang, M. Zhang, T. Niu, A. Li, M. Ye, S. Qiao, G. Ding, X. Xie, Y. Wang, P. K. Chu, Q. Yuan, Z. Di, X. Wang, F. Ding and B. I. Yakobson, *Nano Lett.* **16**, 3160 (2016).
- [22] P. C. Rogge, M. E. Foster, J. M. Wofford, K. F. McCarty, N. C. Bartelt and O. D. Dubon, *MRS Commun.* **5**, 539 (2015).
- [23] L. Gan and Z. Luo, *ACS Nano* **7**, 9480 (2013).
- [24] W. Kern, *J. Electrochem. Soc.* **137**, 1887 (1990).
- [25] S. W. King, R. F. Davis and R. J. Nemanich, *Surf. Sci.* **603**, 3104 (2009).
- [26] S. Shimokawa, A. Namiki, M. N-Gamo and T. Ando, *J. Chem. Phys.* **113**, 6916 (2000).
- [27] J. E. Crowell and G. Lu, *J. Electron. Spectrosc. Relat. Phenom.* **54/55**, 1045 (1990).
- [28] C. Riedl, C. Coletti, T. Iwasaki, A. A. Zakharov and U. Starke, *Phys. Rev. Lett.* **103**, 246804 (2009).
- [29] M. Niwano, M. Terashi and J. Kuge, *Surf. Sci.* **420**, 6 (1999).
- [30] M. Dürr and U. Höfer, *Surf. Sci. Rep.* **61**, 465 (2006).
- [31] M. Dürr, Z. Hu, A. Biedermann, U. Höfer and T. F. Heinz, *Phys. Rev. Lett.* **88**, 046104 (2002).
- [32] F. Speck, J. Jobst, F. Fromm, M. Ostler, D. Waldmann, M. Hundhausen, H. B. Weber and T. Seyller, *Appl. Phys. Lett.* **99**, 122106 (2011).
- [33] N. Sieber, B. F. Mantel, T. Seyller, J. Ristein, L. Ley, T. Heller, D. R. Batchelor and D. Schmeißer, *Appl. Phys. Lett.* **78**, 1216 (2001).
- [34] K. V. Emtsev, A. A. Zakharov, C. Coletti, S. Forti and U. Starke, *Phys. Rev. B* **84**, 125423 (2011).
- [35] E. Aktürk, C. Ataca and S. Ciraci, *Appl. Phys. Lett.* **96**, 123112 (2010).
- [36] D. Ioannis and M. Antonino La, *Appl. Phys. Express* **4**, 125101 (2011).
- [37] J. Tesch, F. Paschke, M. Fonin, M. Wietstruk, S. Bottcher, R. J. Koch, A. Bostwick, C. Jozwiak, E. Rotenberg, A. Makarova, B. Paulus, E. Voloshina and Y. Dedkov, *Nanoscale* **10**, 6088 (2018).
- [38] F. Theilmann, R. Matzdorf, G. Meister and A. Goldmann, *Phys. Rev. B* **56**, 3632 (1997).
- [39] F. Theilmann, R. Matzdorf and A. Goldmann, *Surf. Sci.* **420**, 33 (1999).
- [40] K. R. Knox, A. Locatelli, M. B. Yilmaz, D. Cvetko, T. O. Mentş, M. Á. Niño, P. Kim, A. Morgante and R. M. Osgood, *Phys. Rev. B* **84**, 115401 (2011).